123
8/29/79

LA-7863

MASTER

Lh. 3067

Polarized Triton Elastic Scattering Data

University of California

LOS ALAMOS SCIENTIFIC LABORATORY
Post Office Box 1663 Los Alamos, New Mexico 87545

LA-7863
UC-34c
Issued: July 1979

Polarized Triton Elastic Scattering Data

R. A. Hardekopf
R. F. Haglund, Jr.
G. G. Ohlsen
L. R. Veeser

POLARIZED TRITON ELASTIC SCATTERING DATA

by

R. A. Hardekopf, R. F. Haglund, Jr., G. G. Ohlsen, and L. R. Veeser

ABSTRACT

We measured differential-cross-section and analyzing-power angular distributions for 17-MeV polarized triton elastic scattering. The 13 target nuclei spanned the range $40 \leq A \leq 208$, and the angular range was $20° \leq \theta \leq 160°$. The data are presented in tables and graphs.

I. INTRODUCTION

The installation of a polarized triton ion source at the Los Alamos Scientific Laboratory's tandem Van de Graaff facility has created a unique opportunity to obtain accurate and extensive polarization data for the scattering of tritons from medium and heavy nuclei. A preliminary experiment[1] in 1975 produced the first such data that included scattering angles >60°. The triton bombarding energy was 15 MeV and five target nuclei were studied.

In this experiment, we increased the triton energy to 17 MeV, the maximum available, and studied 13 target nuclei. This report presents tabulated data and some experimental details for this experiment. The interpretation and analysis will be published in Physical Review.[2]

Table I lists the characteristics of the targets used. Figures 1-5 are plots of the data with the optical model (OM) calculations from Ref. 2. The numerical data are tabulated in the Appendix.

II. POLARIZED BEAM

The polarized triton beam was produced in a Lamb-shift polarized ion source[3] and was accelerated by an FN tandem Van de Graaff accelerator.[4] After energy analysis in a 90° bending magnet, the beam was steered into the scattering chamber. The polarized triton source is oriented vertically above the tandem beam line so that a single electrostatic bend deflects the beam into the accelerating tube with the triton quantization axis in the vertical direction. Reversing the guide fields in the polarized ion source reverses the quantization axis so that spin-up and spin-down beams can be produced at the target.

The polarized source has a nuclear spin filter[5] that permits accurate determination of the beam polarization from the atomic beam measurement known as the quench ratio. Briefly, one measures the ratio of the accelerated polarized beam current to the unpolarized current remaining when the dc field in the spin filter is increased enough to "quench" the polarized component of the beam. The procedure is controlled by an on-line computer and the beam currents are read from an integrating digital voltmeter. Tests show that measurements obtained using this method are accurate to within ±0.01.[6] In this experiment, we made such P_Q measurements at the beginning and end of data accumulation runs and at intermediate times during data acquisition for runs longer than 20 min. The average for both spin directions $\bar{P}_Q$ was used as the beam polarization for that run. Variations were within 0.01 during individual runs and <0.05 from beginning to end of the experiment. The average beam polarization was about 0.78.

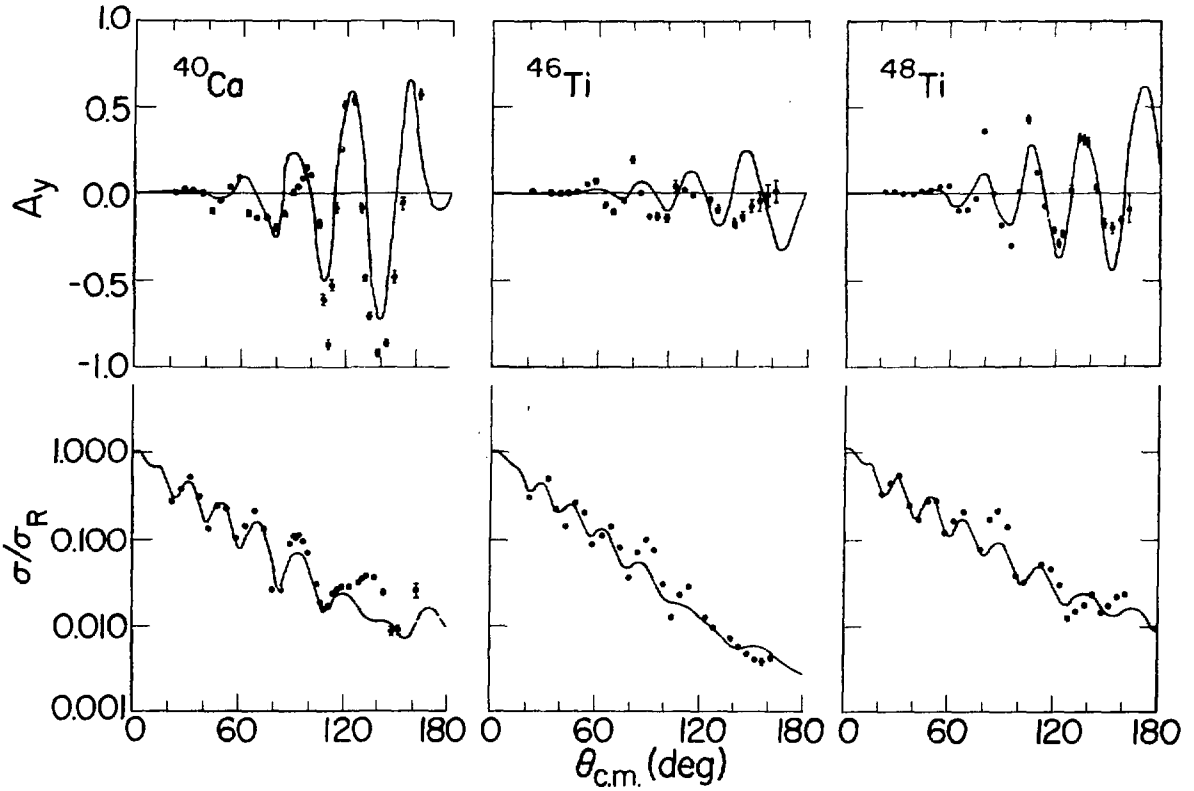

Fig. 1.

Angular distributions of analyzing powers A_y and differential cross sections σ/σ_R (ratio-to-Rutherford) for 17-MeV triton elastic scattering from the three lightest nuclei studied. Error bars are as shown or are smaller than the points. Curves are fits to the data from Ref. 2. The experimental cross sections have been renormalized according to Table I.

The beam was focused to a spot ~2 mm square. Beam intensity available at the target ranged from 20-60 nA during the 11 days of data acquisition. To keep the electronic dead time <10%, we reduced the intensity for forward-angle runs by narrowing a horizontal slit after the 90° analyzing magnet.

The target thicknesses gave energy losses from 0.08-0.39 MeV (Table I). We adjusted the incident beam energy to be 17.0 ± 0.1 MeV at the center of each target.

III. SCATTERING CHAMBER

The scattering chamber was a 61-cm cube[7] with rotatable turntables for mounting detectors in each of four azimuthal quadrants. We used only two turntables, each with two detector telescopes mounted 15° apart. Thus, two pairs of telescopes viewed the target left and right of the beam axis. Each detector assembly consisted of a 300-μm-thick ΔE and a 1000-μm-thick E silicon surface-barrier detector behind a rectangular collimator 3.33 mm wide by 11.4 mm high. The collimator was 241 mm from the target center, giving an angular resolution of ±0.4° and a solid angle of 0.65 msr.

The chamber entrance slits (2.54 mm²) were 60.6 cm from the target center, with exit slits 65.6 cm beyond the center. A beam-position indicator simultaneously displayed the currents intercepted by the first set of entrance slits and by the exit slits. Beam position was maintained by keeping the currents on these slits balanced in the left-right and up-down directions. Currents from the exit slits were

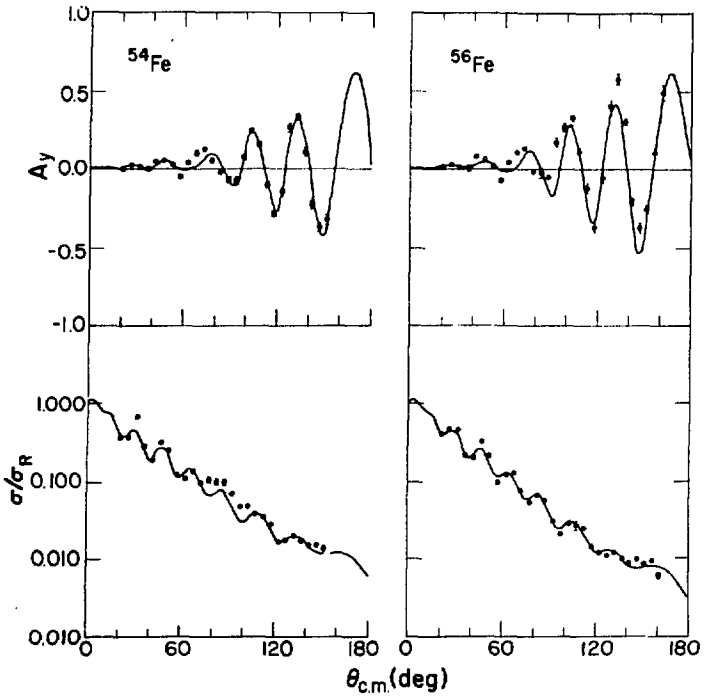

Fig. 2.
Angular distributions of analyzing powers A_y and differential cross sections σ/σ_R for 17-MeV triton elastic scattering from two iron isotopes. See caption for Fig. 1.

added to the Faraday cup current, and the total was recorded by a current integrator.

A mount at the center of the scattering chamber held the target foil either perpendicular to the beam or at a 45° angle for laboratory scattering angles near 90°.

IV. DATA ACQUISITION AND REDUCTION

For coincident ΔE-E events, the linear signals were processed by analog-to-digital converters and were stored in an on-line computer that did the mass identification and recorded the triton pulse-height spectra. We chose gates around an elastic peak and the computer calculated the background by finding a linear fit between a few channels in the valley below and above the peak. For targets with relatively low first excited states (Table I) and for the middle angles, $70° \leq \theta \leq 110°$, where we used the 45° target orientation, spectral broadening from triton energy losses in the target made peak integration imprecise, particularly for detectors facing the side of the target struck by the incident beam. During subsequent analysis of these data, we sometimes used only the spectrum from the telescope that detected scattered tritons transmitted through the target. In these cases, and where there were large backgrounds or the peaks were poorly defined, we increased the assigned relative uncertainties accordingly.

The data acquisition sequence for each angle consisted of runs of equal integrated charge for triton beam polarizations in the up and down directions. Analyzing powers A_y were calculated from the geometric average of left (L) and right (R) detector yields for the two runs.

$$r = \left(\frac{L\uparrow \; R\downarrow}{R\uparrow \; L\downarrow} \right)^{1/2}$$

and

$$A_y = \frac{1}{\bar{P}_Q} \left(\frac{r-1}{r+1} \right) ,$$

where the arrows indicate spin-up and spin-down beam polarizations. This method cancels the effects of differences in detector efficiency and of errors in

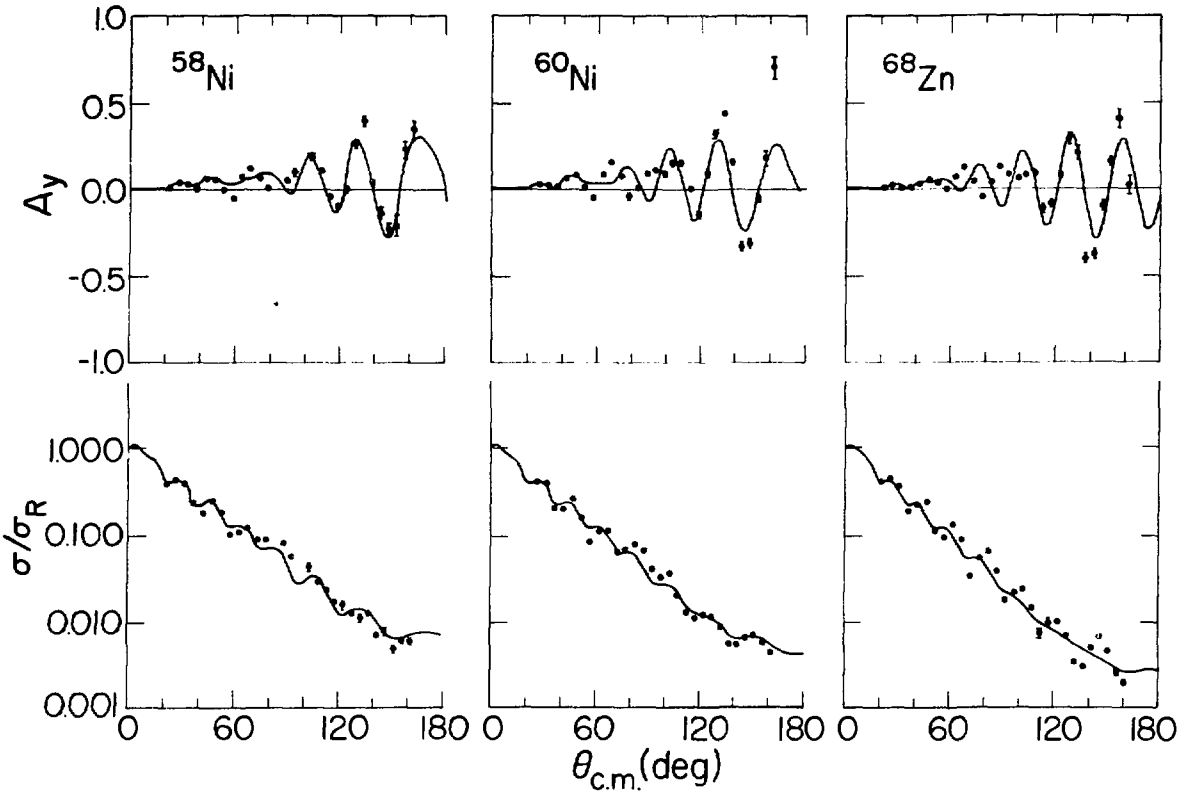

Fig. 3.
Angular distributions of analyzing powers A_y and differential cross sections σ/σ_R for 17-MeV triton elastic scattering from two nickel isotopes and ^{68}Zn. See caption for Fig. 1.

current integration.[8] Data acquisition and processing, quench-ratio measurements, spin-direction control of the polarized source, A_y calculations, and detector angle changes in the scattering chamber were mainly under computer control, so the experimenter could concentrate on setting foreground and background gates in the spectra.

Statistical errors in A_y were from <0.005 at forward angles to ~0.05 at the largest angles. To account for other errors, for example from background determination or beam polarization fluctuations, we combined quadratically a random error of 0.01 with the statistical error to form the total relative error. Besides accounting for experimental uncertainties, this additional error helps to equalize the weighting of points in the angular distribution; otherwise the forward-angle data overly influence the χ^2 minimization procedure used to fit model calculations to the data. The Appendix lists both statistical and total relative errors. The normalization of the analyzing power data, as determined from the quench-ratio beam polarization, is accurate to ±1% of the A_y value. This normalization uncertainty was not included in the errors listed.

For most of the differential-cross-section data the statistical uncertainties in the numbers of counts are small, and other factors are believed to dominate the relative errors. Based on our estimate of the reliability of the current integration and dead-time corrections, relative solid angles, target uniformity, and the quality of the spectra, we assigned a relative error of 5% to most of the cross-section data. We assumed the background determination uncertainty to be 50%, and for those few cases where the background under the peak was >10% of the peak sum, we increased the relative error accordingly.

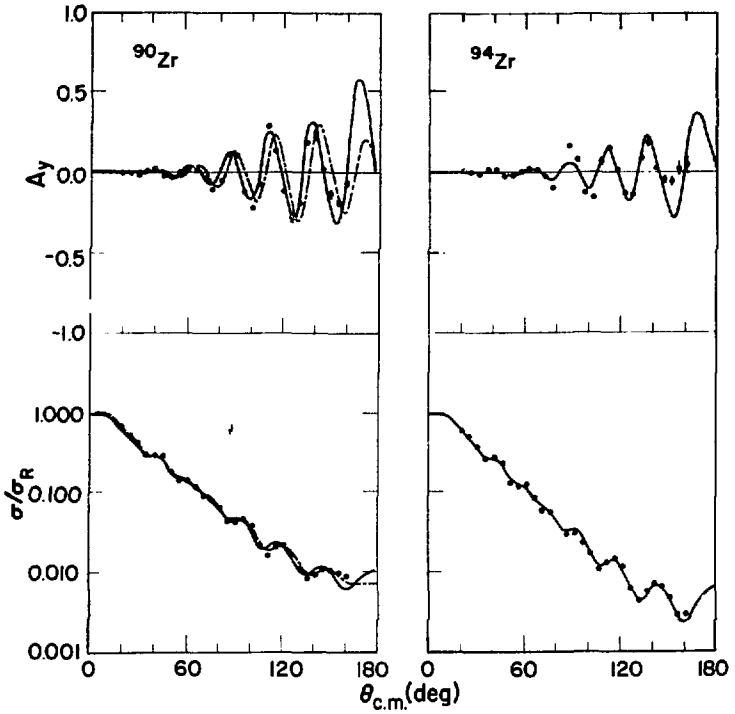

Fig. 4.
Angular distributions of analyzing powers A_y and differential cross sections σ/σ_R for 17-MeV triton elastic scattering from two zirconium isotopes. See caption for Fig. 1.

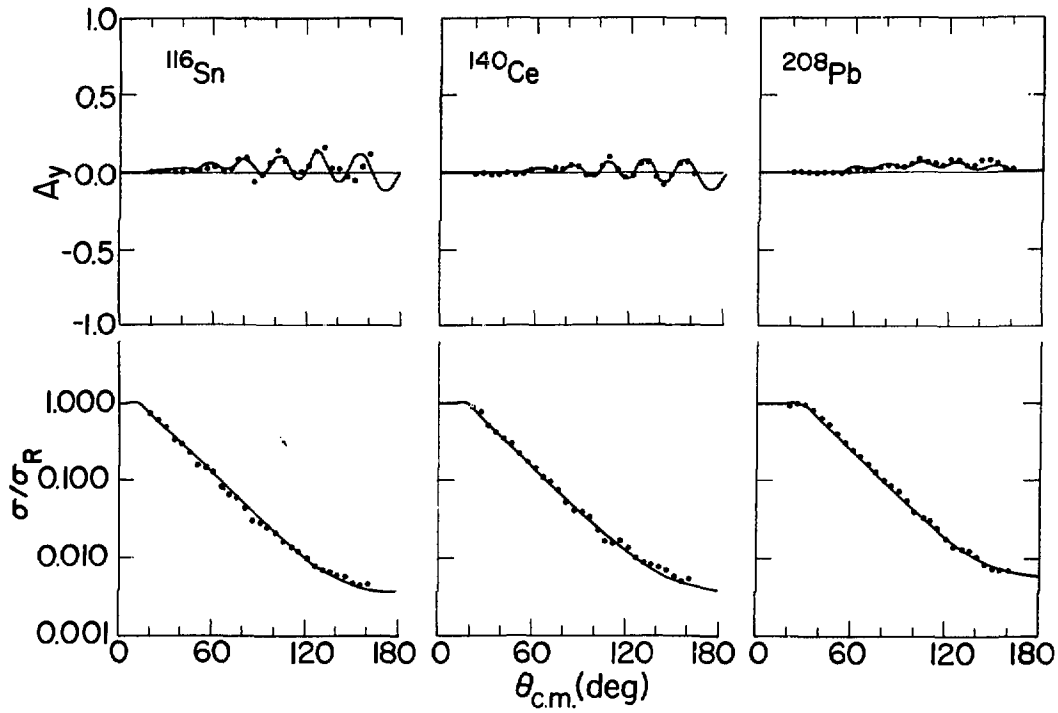

Fig. 5.
Angular distributions of analyzing powers A_y and differential cross sections σ/σ_R for 17-MeV triton elastic scattering from the three heaviest nuclei studied. See caption for Fig. 1.

TABLE I

CHARACTERISTICS OF TARGETS

Target	Target Thickness (mg/cm^2)	ΔE (MeV)[b]	First Excited State (MeV)	Isotopic Purity (%)	OM Renormalization[c]
^{40}Ca	(5.0)[a]	(0.24)	3.35	96.8	1.67
^{46}Ti	5.9	0.25	0.89	81.0	1.15
^{48}Ti	5.7	0.24	0.98	99.6	0.97
^{54}Fe	4.7	0.20	1.41	88.3	1.27
^{56}Fe	4.5	0.19	0.85	99.5	1.17
^{58}Ni	4.1	0.18	1.45	99.3	1.07
^{60}Ni	3.9	0.17	1.33	99.8	1.15
^{68}Zn	4.8	0.20	1.08	98.5	1.16
^{90}Zr	10.8	0.39	1.76	98.1	1.17
^{94}Zr	5.5	0.20	0.92	97.1	1.15
^{116}Sn	8.2	0.28	1.29	(98.0)	1.02
^{140}Ce	6.6	0.20	1.60	88.5	1.29
^{208}Pb	(3.0)	(0.08)	2.61	98.0	0.93

[a]Values in parentheses are estimates.

[b]Energy loss in the target.

[c]Values by which the measurements were multiplied (determined in the analysis of Ref. 2 by minimizing the χ^2_σ values for $\theta \leq 40°$).

Rough normalizations for the differential cross sections were made by measuring or estimating the target thicknesses (Table I) and by calculating the absolute cross sections based on the experimental geometry. Because of the large uncertainties in this procedure (the target uniformity and thicknesses were known only to about 20%), we allowed the overall normalizations of the cross sections to vary during the fitting procedure, renormalizing our data to the OM calculations for $\theta \leq 40°$ where the cross section is dominated by Rutherford scattering and is relatively insensitive to the OM parameters. These renormalization factors, listed in Table I, have been applied to the data tabulations in the Appendix. We assigned a normalization uncertainty of ±10% to each differential-cross-section distribution.

REFERENCES

1. R. A. Hardekopf, L. R. Veeser, and P. W. Keaton, Jr., "Polarization Measurements and Optical-Model Potential for Tritons," Phys. Rev. Lett. **35**, 1623 (1975).

2. R. A. Hardekopf, R. F. Haglund, Jr., G. G. Ohlsen, W. J. Thompson, and L. R. Veeser, "Polarized Triton Elastic Scattering at 17 MeV," Phys. Rev. C(to be published).

3. R. A. Hardekopf, "Operation of the LASL Polarized Triton Source," in *Proceedings of the Fourth International Symposium on Polarization Phenomena in Nuclear Reactions*, Zurich, August 1975, W. Gruebler and V. Konig, Eds. (Birkhauser, Basel, 1976), p. 865.

4. R. Woods, J. L. McKibben, and R. L. Henkel, "The Los Alamos Three-Stage Van de Graaff Facility," Nucl. Instrum. Methods **122**, 81 (1974).

5. G. G. Ohlsen, J. L. McKibben, G. P. Lawrence, P. W. Keaton, Jr., and D. D. Armstrong, "Precise Proton-Polarization Standards Determined with

a Lamb-Shift Ion Source Incorporating a Spin Filter," Phys. Rev. Lett. 27, 599 (1971).

6. R. A. Hardekopf, G. G. Ohlsen, R. V. Poore, and Nelson Jarmie, "Location of a Polarization Extremum in Triton-Alpha Scattering and Its Application to a New Polarized Triton Source," Phys. Rev. C 13, 2127 (1976).

7. G. G. Ohlsen and P. A. Lovoi, "The 'Supercube' Scattering Chamber for Spin-1/2 and Spin-1 Analyzing Power Measurements," in *Proceedings of the Fourth International Symposium on Polarization Phenomena in Nuclear Reactions*, Zurich, August 1975, W. Gruebler and V. Konig, Eds. (Birkhauser, Basel, 1976), p. 907.

8. G. G. Ohlsen and P. W. Keaton, Jr., "Techniques for Measurement of Spin-1/2 and Spin-1 Polarization Analyzing Tensors," Nucl. Instrum. Methods 109, 41 (1973).

APPENDIX

TABULATED DATA FOR TRITON ELASTIC SCATTERING

Numerical data are presented for 17-MeV polarized triton elastic scattering from the 13 target nuclei studied in this experiment. The differential cross section σ is in millibarns per steradian. The ratio-to-Rutherford cross section is σ/σ_r and A_y is the analyzing power which, for elastic scattering, is the same as the polarization. The additional error included for the analyzing power is explained in Sec. IV. The cross sections have been renormalized according to Table I.

$^{40}Ca(t,t)^{40}Ca$ 17 MeV

θ_{cm}	σ	σ/σ_r	$\Delta\sigma$*	A_y	ΔA_y	ΔA_y**
21.49	5.60×10^{2}	3.27×10^{-1}	5.0	−0.002	0.003	0.010
26.84	2.89×10^{2}	4.05×10^{-1}	5.0	0.022	0.002	0.010
32.17	1.89×10^{2}	5.38×10^{-1}	5.0	0.012	0.009	0.013
37.49	6.15×10^{1}	3.16×10^{-1}	5.0	−0.007	0.009	0.013
42.80	1.60×10^{1}	1.37×10^{-1}	5.0	−0.107	0.009	0.013
48.08	1.91×10^{1}	2.54×10^{-1}	5.0	−0.048	0.005	0.011
53.33	1.17×10^{1}	2.30×10^{-1}	5.0	0.032	0.005	0.011
58.56	3.85×10^{0}	1.06×10^{-1}	5.0	0.090	0.008	0.013
63.77	3.85×10^{0}	1.45×10^{-1}	5.0	−0.121	0.011	0.015
68.94	4.36×10^{0}	2.16×10^{-1}	5.0	−0.144	0.008	0.013
74.09	2.11×10^{0}	1.34×10^{-1}	5.0	−0.143	0.011	0.015
79.20	3.31×10^{-1}	2.63×10^{-2}	5.0	−0.196	0.017	0.020
84.28	2.72×10^{-1}	2.66×10^{-2}	5.0	−0.120	0.018	0.021
89.33	7.76×10^{-1}	9.14×10^{-2}	5.0	0.005	0.009	0.013
91.84	8.77×10^{-1}	1.13×10^{-1}	5.0	0.037	0.010	0.014
94.35	8.14×10^{-1}	1.14×10^{-1}	5.0	0.089	0.010	0.014
96.84	6.38×10^{-1}	9.64×10^{-2}	5.0	0.148	0.012	0.016
99.33	4.35×10^{-1}	7.09×10^{-2}	5.0	0.104	0.014	0.017
104.28	1.61×10^{-1}	3.03×10^{-2}	5.0	−0.178	0.021	0.023
106.74	9.53×10^{-2}	1.91×10^{-2}	5.0	−0.617	0.030	0.032
109.20	7.41×10^{-2}	1.58×10^{-2}	5.0	−0.875	0.026	0.028
111.65	7.44×10^{-2}	1.68×10^{-2}	5.0	−0.529	0.035	0.036
114.09	9.93×10^{-2}	2.38×10^{-2}	5.0	−0.087	0.025	0.027
116.51	1.07×10^{-1}	2.71×10^{-2}	5.0	0.257	0.019	0.021
118.94	1.07×10^{-1}	2.85×10^{-2}	5.0	0.516	0.019	0.021
123.77	9.58×10^{-2}	2.80×10^{-2}	5.0	0.537	0.025	0.027
128.56	1.00×10^{-1}	3.18×10^{-2}	5.0	−0.090	0.025	0.027
130.94	1.04×10^{-1}	3.44×10^{-2}	5.0	−0.486	0.019	0.021
133.33	1.09×10^{-1}	3.73×10^{-2}	5.0	−0.715	0.018	0.021
138.07	9.93×10^{-2}	3.64×10^{-2}	5.0	−0.925	0.015	0.018
142.79	6.27×10^{-2}	2.44×10^{-2}	6.0	−0.871	0.017	0.020
147.49	2.17×10^{-2}	8.90×10^{-3}	12.5	−0.482	0.038	0.039
152.17	2.14×10^{-2}	9.18×10^{-3}	15.0	−0.057	0.037	0.038
161.49	5.70×10^{-2}	2.61×10^{-2}	20.0	0.572	0.028	0.030

* relative percentage error
** total error including 0.01 random error

$^{46}Ti(t,t)^{46}Ti$ 17 MeV

θ_{cm}	σ	σ/σ_r	$\Delta\sigma$*	A_y	ΔA_y	ΔA_y**
21.29	7.20×10^{2}	3.40×10^{-1}	5.0	0.006	0.002	0.010
31.89	2.20×10^{2}	5.09×10^{-1}	5.0	0.002	0.004	0.011
37.17	5.51×10^{1}	2.31×10^{-1}	5.0	−0.009	0.005	0.011
42.43	2.05×10^{1}	1.43×10^{-1}	5.0	−0.008	0.006	0.012
47.67	2.44×10^{1}	2.64×10^{-1}	5.0	0.006	0.004	0.011
52.90	1.30×10^{1}	2.07×10^{-1}	5.0	0.048	0.006	0.012
58.10	3.91×10^{0}	8.82×10^{-2}	5.0	0.068	0.013	0.016
63.28	3.64×10^{0}	1.12×10^{-1}	5.0	−0.071	0.012	0.016
68.43	3.45×10^{0}	1.40×10^{-1}	5.0	−0.112	0.012	0.016
73.56	1.53×10^{0}	7.99×10^{-2}	5.0	−0.047	0.015	0.018
78.65	5.34×10^{-1}	3.50×10^{-2}	5.0	0.198	0.018	0.021
83.73	8.76×10^{-1}	7.06×10^{-2}	5.0	−0.004	0.008	0.013
88.77	1.03×10^{0}	9.97×10^{-2}	5.0	−0.140	0.007	0.012
93.78	6.40×10^{-1}	7.38×10^{-2}	5.0	−0.139	0.017	0.020
98.77	2.22×10^{-1}	2.99×10^{-2}	5.0	−0.148	0.016	0.019
103.73	8.13×10^{-2}	1.26×10^{-2}	5.0	0.040	0.029	0.031
108.65	1.27×10^{-1}	2.24×10^{-2}	5.0	0.013	0.011	0.015
113.55	1.37×10^{-1}	2.72×10^{-2}	5.0	−0.021	0.010	0.014
123.28	5.07×10^{-2}	1.24×10^{-2}	5.0	−0.045	0.017	0.020
128.10	3.60×10^{-2}	9.55×10^{-3}	5.0	−0.096	0.020	0.022
137.67	2.38×10^{-2}	7.31×10^{-3}	5.0	−0.179	0.023	0.025
142.43	1.78×10^{-2}	5.79×10^{-3}	5.0	−0.135	0.033	0.034
147.17	1.38×10^{-2}	4.76×10^{-3}	5.0	−0.077	0.040	0.041
151.89	1.13×10^{-2}	4.05×10^{-3}	6.7	−0.049	0.059	0.060
156.60	1.01×10^{-2}	3.77×10^{-3}	7.9	−0.018	0.069	0.070
161.29	1.12×10^{-2}	4.30×10^{-3}	7.5	0.010	0.071	0.072

* relative percentage error
** total error including 0.01 random error

$^{48}Ti(t,t)^{48}Ti$ 17 MeV

θ_{cm}	σ	σ/σ_r	$\Delta\sigma$*	A_y	ΔA_y	ΔA_y**
21.25	7.67×10^{2}	3.62×10^{-1}	5.0	0.012	0.004	0.011
26.55	3.91×10^{2}	4.43×10^{-1}	5.0	0.013	0.002	0.010
31.80	2.29×10^{2}	5.25×10^{-1}	5.0	−0.004	0.002	0.010
37.10	5.76×10^{1}	2.41×10^{-1}	5.0	−0.005	0.004	0.011
42.35	2.42×10^{1}	1.68×10^{-1}	5.0	0.016	0.006	0.012
47.55	2.53×10^{1}	2.73×10^{-1}	5.0	0.020	0.007	0.012
52.80	1.69×10^{1}	2.69×10^{-1}	5.0	0.040	0.010	0.014
57.95	5.12×10^{0}	1.15×10^{-1}	5.0	0.046	0.010	0.014
63.15	5.22×10^{0}	1.60×10^{-1}	5.0	−0.102	0.008	0.013
68.30	5.00×10^{0}	2.03×10^{-1}	5.0	−0.098	0.009	0.013
78.50	1.14×10^{0}	7.43×10^{-2}	5.0	0.367	0.009	0.013
83.55	2.04×10^{0}	1.64×10^{-1}	5.0	−0.007	0.007	0.012
88.60	2.15×10^{0}	2.09×10^{-1}	5.0	−0.186	0.005	0.011
93.65	1.19×10^{0}	1.38×10^{-1}	5.0	−0.302	0.007	0.012
98.60	2.65×10^{-1}	3.57×10^{-2}	5.0	0.007	0.007	0.012
103.55	1.89×10^{-1}	2.93×10^{-2}	5.0	0.428	0.016	0.019
113.40	2.50×10^{-1}	4.98×10^{-2}	5.0	−0.078	0.010	0.014
118.30	1.95×10^{-1}	4.33×10^{-2}	5.0	−0.212	0.013	0.016
123.15	1.14×10^{-1}	2.79×10^{-2}	5.0	−0.232	0.012	0.016
127.95	4.49×10^{-2}	1.12×10^{-2}	5.0	0.014	0.027	0.029
132.80	5.02×10^{-2}	1.44×10^{-2}	5.0	0.323	0.025	0.027
137.55	5.37×10^{-2}	1.65×10^{-2}	5.0	0.294	0.024	0.026
142.35	6.67×10^{-2}	2.19×10^{-2}	5.0	0.029	0.017	0.020
147.10	3.91×10^{-2}	1.35×10^{-2}	5.0	−0.180	0.025	0.027
151.80	4.49×10^{-2}	1.62×10^{-2}	5.0	−0.204	0.027	0.029
156.55	5.48×10^{-2}	2.06×10^{-2}	5.0	−0.158	0.018	0.021
161.25	5.73×10^{-2}	2.22×10^{-2}	10.0	−0.095	0.076	0.077

* relative percentage error
** total error including 0.01 random error

$^{54}Fe(t,t)^{54}Fe$ 17 MeV

θ_{cm}	σ	σ/σ_r	$\Delta\sigma$*	A_y	ΔA_y	ΔA_y**
21.10	1.17×10^{3}	3.90×10^{-1}	5.0	−0.004	0.002	0.010
26.36	4.64×10^{2}	3.71×10^{-1}	5.0	0.021	0.002	0.010
31.61	4.02×10^{2}	6.55×10^{-1}	5.0	0.010	0.008	0.013
36.85	9.31×10^{1}	2.75×10^{-1}	5.0	0.002	0.006	0.012
42.07	3.84×10^{1}	1.89×10^{-1}	5.0	0.045	0.007	0.012
47.28	4.05×10^{1}	3.10×10^{-1}	5.0	0.054	0.007	0.012
52.47	2.21×10^{1}	2.49×10^{-1}	5.0	0.019	0.006	0.012
57.64	7.48×10^{0}	1.20×10^{-1}	5.0	−0.057	0.007	0.012
62.79	5.17×10^{0}	1.13×10^{-1}	5.0	0.038	0.009	0.013
67.92	4.64×10^{0}	1.34×10^{-1}	5.0	0.096	0.009	0.013
73.03	2.66×10^{0}	9.86×10^{-2}	5.0	0.130	0.012	0.016
78.11	2.32×10^{0}	1.08×10^{-1}	7.5	0.052	0.014	0.017
83.17	1.75×10^{0}	1.01×10^{-1}	7.5	−0.025	0.007	0.012
88.21	1.43×10^{0}	9.92×10^{-2}	7.5	−0.071	0.007	0.012
93.22	8.45×10^{-1}	6.98×10^{-2}	5.0	−0.074	0.013	0.016
98.21	4.94×10^{-1}	4.77×10^{-2}	5.0	0.070	0.012	0.016
103.17	4.32×10^{-1}	4.82×10^{-2}	5.0	0.248	0.013	0.016
108.11	3.02×10^{-1}	3.83×10^{-2}	5.0	0.157	0.009	0.013
113.03	2.44×10^{-1}	3.49×10^{-2}	5.0	−0.106	0.010	0.014
117.92	1.74×10^{-1}	2.77×10^{-2}	5.0	−0.277	0.012	0.016
122.79	9.28×10^{-2}	1.63×10^{-2}	5.0	−0.147	0.018	0.021
127.64	8.84×10^{-2}	1.70×10^{-2}	7.5	0.274	0.027	0.029
132.47	9.16×10^{-2}	1.90×10^{-2}	5.0	0.342	0.016	0.019
137.28	7.42×10^{-2}	1.65×10^{-2}	5.0	0.110	0.022	0.024
142.07	6.18×10^{-2}	1.46×10^{-2}	5.0	−0.228	0.025	0.027
146.85	5.91×10^{-2}	1.48×10^{-2}	5.0	−0.375	0.026	0.028
151.61	5.03×10^{-2}	1.31×10^{-2}	10.0	−0.325	0.032	0.034

* relative percentage error
** total error including 0.01 random error

$^{56}Fe(t,t)^{56}Fe$ 17 MeV

θ_{cm}	σ	σ/σ_r	$\Delta\sigma$*	A_y	ΔA_y	ΔA_y**
21.06	1.26×10^{3}	4.18×10^{-1}	5.0	0.005	0.003	0.010
26.31	5.73×10^{2}	4.57×10^{-1}	5.0	0.021	0.003	0.010
31.55	2.67×10^{2}	4.33×10^{-1}	5.0	0.003	0.009	0.013
36.78	7.03×10^{1}	2.07×10^{-1}	5.0	−0.004	0.011	0.015
42.00	3.90×10^{1}	1.91×10^{-1}	5.0	0.075	0.011	0.015
47.20	3.96×10^{1}	3.02×10^{-1}	5.0	0.061	0.003	0.010
52.38	1.79×10^{1}	2.02×10^{-1}	5.0	0.016	0.003	0.010
57.55	5.90×10^{0}	9.42×10^{-2}	5.0	−0.080	0.005	0.011
62.69	5.43×10^{0}	1.18×10^{-1}	5.0	0.037	0.007	0.012
67.82	4.25×10^{0}	1.22×10^{-1}	5.0	0.105	0.006	0.012
72.92	1.97×10^{0}	7.32×10^{-2}	5.0	0.133	0.009	0.013
78.00	1.10×10^{0}	5.15×10^{-2}	5.0	−0.023	0.017	0.020
83.06	1.15×10^{0}	6.59×10^{-2}	5.0	−0.036	0.014	0.017
88.10	7.94×10^{-1}	5.52×10^{-2}	5.0	−0.059	0.016	0.019
93.11	3.54×10^{-1}	2.93×10^{-2}	5.0	0.167	0.022	0.024
98.10	2.02×10^{-1}	1.95×10^{-2}	5.0	0.272	0.025	0.027
103.06	2.45×10^{-1}	2.74×10^{-2}	5.0	0.333	0.015	0.018
108.00	2.04×10^{-1}	2.59×10^{-2}	10.0	0.109	0.015	0.018
112.92	1.63×10^{-1}	2.34×10^{-2}	5.0	−0.128	0.025	0.027
117.82	8.53×10^{-2}	1.36×10^{-2}	5.0	−0.372	0.028	0.030
122.69	6.41×10^{-2}	1.13×10^{-2}	5.0	−0.063	0.030	0.032
127.54	5.43×10^{-2}	1.05×10^{-2}	5.0	0.408	0.031	0.033
132.38	5.40×10^{-2}	1.12×10^{-2}	5.0	0.577	0.031	0.033
137.20	4.22×10^{-2}	9.43×10^{-3}	5.0	0.304	0.019	0.021
142.00	3.45×10^{-2}	8.20×10^{-3}	5.0	−0.211	0.021	0.023
146.78	3.69×10^{-2}	9.25×10^{-3}	5.0	−0.377	0.031	0.033
151.55	3.04×10^{-2}	7.98×10^{-3}	5.0	−0.259	0.025	0.027
156.31	3.25×10^{-2}	8.85×10^{-3}	5.0	0.099	0.027	0.029
161.06	2.07×10^{-2}	5.82×10^{-3}	5.0	0.494	0.050	0.051

* relative percentage error
** total error including 0.01 random error

$^{58}Ni(t,t)^{58}Ni$ 17 MeV

θ_{cm}	σ	σ/σ_r	$\Delta\sigma$*	A_y	ΔA_y	ΔA_y**
21.03	1.56×10^{3}	4.45×10^{-1}	5.0	0.003	0.005	0.011
26.27	6.61×10^{2}	4.53×10^{-1}	5.0	0.031	0.005	0.011
31.50	2.90×10^{2}	4.05×10^{-1}	5.0	0.021	0.004	0.011
36.72	9.44×10^{1}	2.39×10^{-1}	7.5	0.006	0.021	0.023
41.93	4.37×10^{1}	1.84×10^{-1}	5.0	0.060	0.006	0.012
47.12	3.90×10^{1}	2.56×10^{-1}	5.0	0.054	0.003	0.010
52.30	1.89×10^{1}	1.84×10^{-1}	5.0	−0.009	0.003	0.010
57.46	7.41×10^{0}	1.02×10^{-1}	5.0	−0.055	0.005	0.011
62.60	5.72×10^{0}	1.07×10^{-1}	5.0	0.069	0.008	0.013
67.72	4.98×10^{0}	1.23×10^{-1}	5.0	0.116	0.009	0.013
72.82	2.76×10^{0}	8.82×10^{-2}	5.0	0.066	0.008	0.013
77.90	2.19×10^{0}	8.80×10^{-2}	5.0	0.003	0.009	0.013
87.99	1.34×10^{0}	8.00×10^{-2}	5.0	0.044	0.011	0.015
93.00	7.84×10^{-1}	5.58×10^{-2}	5.0	0.096	0.015	0.018
102.95	4.40×10^{-1}	4.23×10^{-2}	7.5	0.190	0.021	0.023
107.90	2.58×10^{-1}	2.84×10^{-2}	5.0	0.104	0.011	0.015
112.82	1.87×10^{-1}	2.31×10^{-2}	5.0	−0.045	0.012	0.016
117.72	1.23×10^{-1}	1.69×10^{-2}	5.0	−0.102	0.012	0.016
122.60	1.05×10^{-1}	1.60×10^{-2}	10.0	−0.004	0.017	0.020
127.46	7.65×10^{-2}	1.27×10^{-2}	7.5	0.261	0.025	0.027
132.30	6.30×10^{-2}	1.13×10^{-2}	7.5	0.392	0.024	0.026
137.12	6.76×10^{-2}	1.31×10^{-2}	7.5	0.034	0.021	0.023
141.93	3.54×10^{-2}	7.26×10^{-3}	7.5	−0.136	0.036	0.037
146.72	3.75×10^{-2}	8.13×10^{-3}	7.5	−0.229	0.032	0.034
151.50	2.17×10^{-2}	4.92×10^{-3}	7.5	−0.206	0.057	0.058
156.27	2.66×10^{-2}	6.28×10^{-3}	7.5	0.229	0.051	0.052
161.03	2.55×10^{-2}	6.19×10^{-3}	7.5	0.346	0.052	0.053

* relative percentage error
** total error including 0.01 random error

$^{60}Ni(t,t)^{60}Ni$ 17 MeV

θ_{cm}	σ	σ/σ_r	$\Delta\sigma$*	A_y	ΔA_y	ΔA_y**
26.23	6.47×10^{2}	4.42×10^{-1}	5.0	0.024	0.005	0.011
31.45	2.99×10^{2}	4.16×10^{-1}	5.0	0.016	0.004	0.011
36.66	8.38×10^{1}	2.11×10^{-1}	5.0	0.008	0.004	0.011
41.86	4.88×10^{1}	2.05×10^{-1}	7.5	0.062	0.017	0.020
47.05	4.12×10^{1}	2.70×10^{-1}	5.0	0.075	0.011	0.015
52.22	1.70×10^{1}	1.65×10^{-1}	5.0	0.011	0.008	0.013
57.38	6.18×10^{0}	8.46×10^{-2}	5.0	−0.052	0.006	0.012
62.51	6.10×10^{0}	1.14×10^{-1}	5.0	0.079	0.010	0.014
67.63	4.62×10^{0}	1.14×10^{-1}	5.0	0.152	0.007	0.012
72.73	2.01×10^{0}	6.42×10^{-2}	5.0	0.074	0.011	0.015
77.80	1.69×10^{0}	6.80×10^{-2}	5.0	−0.045	0.009	0.013
82.86	1.59×10^{0}	7.88×10^{-2}	5.0	0.006	0.007	0.012
87.89	1.12×10^{0}	6.70×10^{-2}	5.0	0.089	0.007	0.012
92.90	5.82×10^{-1}	4.14×10^{-2}	5.0	0.110	0.015	0.018
97.89	3.90×10^{-1}	3.25×10^{-2}	5.0	0.090	0.015	0.018
102.86	3.76×10^{-1}	3.62×10^{-2}	5.0	0.153	0.013	0.016
107.80	1.86×10^{-1}	2.05×10^{-2}	5.0	0.155	0.015	0.018
112.73	1.08×10^{-1}	1.34×10^{-2}	5.0	0.002	0.016	0.019
117.63	8.13×10^{-2}	1.12×10^{-2}	5.0	−0.150	0.014	0.017
122.51	8.05×10^{-2}	1.23×10^{-2}	5.0	0.093	0.023	0.025
127.38	7.01×10^{-2}	1.17×10^{-2}	5.0	0.328	0.020	0.022
132.22	4.95×10^{-2}	8.92×10^{-3}	5.0	0.440	0.017	0.020
137.05	2.93×10^{-2}	5.66×10^{-3}	5.0	0.162	0.017	0.020
141.86	2.75×10^{-2}	5.65×10^{-3}	5.0	−0.329	0.023	0.025
146.66	3.14×10^{-2}	6.83×10^{-3}	5.0	−0.310	0.022	0.024
151.45	3.18×10^{-2}	7.23×10^{-3}	5.0	−0.054	0.022	0.024
156.23	2.56×10^{-2}	6.07×10^{-3}	7.5	0.181	0.046	0.047
160.99	1.91×10^{-2}	4.67×10^{-3}	7.5	0.702	0.066	0.067

* relative percentage error
** total error including 0.01 random error

$^{68}Zn(t,t)^{68}Zn$ 17 MeV

θ_{cm}	σ	σ/σ_r	$\Delta\sigma$*	A_y	ΔA_y	ΔA_y**
20.88	1.84×10^{3}	4.52×10^{-1}	5.0	0.006	0.003	0.010
26.08	7.96×10^{2}	4.69×10^{-1}	5.0	0.022	0.002	0.010
31.28	3.11×10^{2}	3.73×10^{-1}	5.0	−0.001	0.010	0.014
36.47	8.92×10^{1}	1.94×10^{-1}	5.0	0.004	0.012	0.016
41.64	6.37×10^{1}	2.31×10^{-1}	5.0	0.027	0.008	0.013
46.81	4.36×10^{1}	2.47×10^{-1}	5.0	0.053	0.004	0.011
51.96	1.34×10^{1}	1.12×10^{-1}	5.0	0.032	0.005	0.011
57.10	7.91×10^{0}	9.38×10^{-2}	5.0	−0.005	0.005	0.011
62.22	8.52×10^{0}	1.38×10^{-1}	5.0	0.070	0.008	0.013
67.32	4.12×10^{0}	8.85×10^{-2}	5.0	0.124	0.009	0.013
72.40	1.18×10^{0}	3.26×10^{-2}	5.0	0.041	0.012	0.016
77.47	1.54×10^{0}	5.37×10^{-2}	5.0	−0.050	0.008	0.013
82.52	1.48×10^{0}	6.37×10^{-2}	5.0	0.038	0.006	0.012
87.55	7.18×10^{-1}	3.74×10^{-2}	5.0	0.130	0.007	0.012
92.56	2.84×10^{-1}	1.76×10^{-2}	10.0	0.086	0.020	0.022
97.55	2.90×10^{-1}	2.11×10^{-2}	5.0	0.061	0.011	0.015
102.52	2.82×10^{-1}	2.37×10^{-2}	5.0	0.080	0.010	0.014
107.47	1.49×10^{-1}	1.43×10^{-2}	5.0	0.091	0.014	0.017
112.40	6.87×10^{-2}	7.45×10^{-3}	10.0	−0.114	0.023	0.025
117.32	8.11×10^{-2}	9.81×10^{-3}	10.0	−0.088	0.020	0.022
122.22	7.54×10^{-2}	1.01×10^{-2}	5.0	0.079	0.022	0.024
127.10	4.66×10^{-2}	6.81×10^{-3}	5.0	0.294	0.032	0.034
131.96	2.18×10^{-2}	3.45×10^{-3}	5.0	0.208	0.037	0.038
136.81	1.79×10^{-2}	3.04×10^{-3}	5.0	−0.398	0.030	0.032
141.64	2.79×10^{-2}	5.05×10^{-3}	5.0	−0.370	0.032	0.034
146.47	3.49×10^{-2}	6.67×10^{-3}	5.0	−0.099	0.028	0.030
151.28	2.33×10^{-2}	4.67×10^{-3}	5.0	0.160	0.023	0.025
156.08	1.23×10^{-2}	2.57×10^{-3}	10.0	0.406	0.059	0.060
160.87	9.05×10^{-3}	1.95×10^{-3}	10.0	0.021	0.055	0.056

* relative percentage error
** total error including 0.01 random error

$^{90}Zr(t,t)^{90}Zr$ 17 MeV

θ_{cm}	σ	σ/σ_r	$\Delta\sigma$*	A_y	ΔA_y	ΔA_y**
20.66	5.21×10^{3}	7.03×10^{-1}	10.0	−0.004	0.002	0.010
25.82	1.59×10^{3}	5.16×10^{-1}	5.0	−0.003	0.002	0.010
30.97	6.26×10^{2}	4.15×10^{-1}	5.0	−0.016	0.004	0.011
36.11	2.36×10^{2}	2.84×10^{-1}	5.0	0.010	0.004	0.011
41.24	1.38×10^{2}	2.76×10^{-1}	5.0	0.019	0.003	0.010
46.37	8.57×10^{1}	2.69×10^{-1}	5.0	−0.026	0.003	0.010
51.48	3.63×10^{1}	1.68×10^{-1}	5.0	−0.036	0.005	0.011
56.58	1.95×10^{1}	1.28×10^{-1}	5.0	0.000	0.004	0.011
61.67	1.45×10^{1}	1.30×10^{-1}	5.0	0.017	0.006	0.012
66.75	9.10×10^{0}	1.09×10^{-1}	5.0	0.013	0.010	0.014
71.82	5.40×10^{0}	8.34×10^{-2}	5.0	−0.039	0.008	0.013
76.87	3.93×10^{0}	7.66×10^{-2}	5.0	−0.111	0.006	0.012
81.90	2.48×10^{0}	5.96×10^{-2}	5.0	−0.055	0.007	0.012
86.93	1.42×10^{0}	4.16×10^{-2}	5.0	0.110	0.008	0.013
91.93	1.15×10^{0}	4.00×10^{-2}	5.0	0.104	0.010	0.014
96.93	1.07×10^{0}	4.37×10^{-2}	5.0	−0.126	0.011	0.015
101.90	7.56×10^{-1}	3.59×10^{-2}	5.0	−0.236	0.010	0.014
106.87	3.84×10^{-1}	2.09×10^{-2}	5.0	−0.083	0.009	0.013
111.82	2.51×10^{-1}	1.54×10^{-2}	5.0	0.281	0.012	0.016
116.75	2.90×10^{-1}	1.99×10^{-2}	5.0	0.128	0.009	0.013
121.67	2.68×10^{-1}	2.04×10^{-2}	5.0	−0.130	0.011	0.015
126.58	1.84×10^{-1}	1.53×10^{-2}	5.0	−0.307	0.013	0.016
131.48	1.15×10^{-1}	1.03×10^{-2}	5.0	−0.207	0.014	0.017
136.37	8.00×10^{-2}	7.75×10^{-3}	5.0	0.180	0.018	0.021
141.24	8.32×10^{-2}	8.60×10^{-3}	5.0	0.218	0.018	0.021
146.11	9.02×10^{-2}	9.85×10^{-3}	5.0	0.014	0.017	0.020
150.97	8.58×10^{-2}	9.84×10^{-3}	5.0	−0.144	0.018	0.021
155.82	7.53×10^{-2}	8.99×10^{-3}	5.0	−0.208	0.020	0.022
160.66	6.57×10^{-2}	8.09×10^{-3}	5.0	−0.076	0.023	0.025

* relative percentage error
** total error including 0.01 random error

$^{94}Zr(t,t)^{94}Zr$ 17 MeV

θ_{cm}	σ	σ/σ_r	$\Delta\sigma$*	A_y	ΔA_y	ΔA_y**
20.63	4.63×10^{0}	6.22×10^{-1}	5.0	0.008	0.002	0.010
25.78	1.63×10^{0}	5.28×10^{-1}	5.0	−0.001	0.002	0.010
30.93	5.64×10^{-1}	3.73×10^{-1}	5.0	−0.012	0.009	0.013
36.06	2.12×10^{-1}	2.54×10^{-1}	5.0	0.022	0.008	0.013
41.19	1.35×10^{-1}	2.71×10^{-1}	5.0	0.016	0.007	0.012
46.31	7.13×10^{-2}	2.23×10^{-1}	5.0	−0.026	0.003	0.010
51.42	2.71×10^{-2}	1.26×10^{-1}	5.0	−0.022	0.004	0.011
56.52	1.74×10^{-2}	1.15×10^{-1}	5.0	0.000	0.004	0.011
61.60	1.34×10^{-2}	1.21×10^{-1}	5.0	0.025	0.007	0.012
66.68	6.97×10^{-3}	8.32×10^{-2}	5.0	0.022	0.008	0.013
71.74	3.80×10^{-3}	5.87×10^{-2}	5.0	−0.026	0.008	0.013
76.79	2.83×10^{-3}	5.51×10^{-2}	5.0	−0.100	0.007	0.012
86.84	1.01×10^{-3}	2.95×10^{-2}	5.0	0.167	0.015	0.018
91.85	8.59×10^{-4}	3.00×10^{-2}	5.0	0.082	0.013	0.016
96.84	5.70×10^{-4}	2.34×10^{-2}	6.0	−0.130	0.020	0.022
101.82	3.69×10^{-4}	1.75×10^{-2}	5.0	−0.160	0.016	0.019
106.79	2.01×10^{-4}	1.09×10^{-2}	5.0	0.067	0.020	0.022
111.74	2.10×10^{-4}	1.29×10^{-2}	5.0	0.152	0.013	0.016
116.68	2.14×10^{-4}	1.47×10^{-2}	5.0	0.015	0.013	0.016
121.60	1.50×10^{-4}	1.14×10^{-2}	5.0	−0.137	0.015	0.018
126.52	7.37×10^{-5}	6.13×10^{-3}	5.0	−0.142	0.022	0.024
131.42	4.79×10^{-5}	4.33×10^{-3}	5.0	0.083	0.028	0.030
136.31	5.70×10^{-5}	5.54×10^{-3}	5.0	0.190	0.020	0.022
141.19	6.89×10^{-5}	7.14×10^{-3}	5.0	0.028	0.018	0.021
146.06	5.86×10^{-5}	6.42×10^{-3}	5.0	−0.043	0.020	0.022
150.93	3.93×10^{-5}	4.52×10^{-3}	5.0	−0.055	0.024	0.026
155.78	2.46×10^{-5}	2.95×10^{-3}	13.0	0.026	0.041	0.042
160.63	2.32×10^{-5}	2.86×10^{-3}	22.0	0.051	0.052	0.053

* relative percentage error
** total error including 0.01 random error

$^{116}Sn(t,t)^{116}Sn$ 17 MeV

θ_{cm}	σ	σ/σ_r	$\Delta\sigma$*	A_y	ΔA_y	ΔA_y**
20.51	9.24×10^{0}	7.87×10^{-1}	5.0	0.003	0.005	0.011
25.63	3.01×10^{0}	6.18×10^{-1}	5.0	0.005	0.005	0.011
30.75	1.18×10^{0}	4.94×10^{-1}	5.0	0.006	0.005	0.011
35.86	4.35×10^{-1}	3.31×10^{-1}	5.0	0.000	0.003	0.010
40.96	2.25×10^{-1}	2.86×10^{-1}	5.0	0.006	0.003	0.010
46.06	1.11×10^{-1}	2.21×10^{-1}	5.0	0.012	0.003	0.010
51.15	5.21×10^{-2}	1.53×10^{-1}	5.0	0.019	0.004	0.011
56.23	3.41×10^{-2}	1.43×10^{-1}	5.0	0.027	0.004	0.011
61.30	2.17×10^{-2}	1.24×10^{-1}	5.0	0.036	0.006	0.012
66.36	1.08×10^{-2}	8.21×10^{-2}	5.0	0.011	0.009	0.013
71.41	6.53×10^{-3}	6.42×10^{-2}	5.0	0.026	0.008	0.013
76.45	4.68×10^{-3}	5.81×10^{-2}	5.0	0.089	0.005	0.011
81.48	2.91×10^{-3}	4.47×10^{-2}	5.0	0.095	0.005	0.011
86.49	1.61×10^{-3}	3.02×10^{-2}	5.0	−0.064	0.008	0.013
91.50	1.27×10^{-3}	2.84×10^{-2}	5.0	−0.014	0.009	0.013
96.49	9.79×10^{-4}	2.57×10^{-2}	5.0	0.061	0.008	0.013
101.48	6.76×10^{-4}	2.06×10^{-2}	5.0	0.147	0.012	0.016
106.45	4.71×10^{-4}	1.64×10^{-2}	5.0	0.076	0.011	0.015
111.41	3.41×10^{-4}	1.35×10^{-2}	5.0	0.005	0.012	0.016
116.36	2.71×10^{-4}	1.20×10^{-2}	5.0	−0.001	0.012	0.016
121.30	2.01×10^{-4}	9.84×10^{-3}	5.0	0.042	0.018	0.021
126.23	1.42×10^{-4}	7.62×10^{-3}	5.0	0.137	0.019	0.021
131.15	1.14×10^{-4}	6.66×10^{-3}	5.0	0.167	0.019	0.021
136.06	1.01×10^{-4}	6.32×10^{-3}	5.0	0.027	0.018	0.021
140.96	8.38×10^{-5}	5.61×10^{-3}	5.0	0.025	0.020	0.022
145.86	7.62×10^{-5}	5.39×10^{-3}	5.0	−0.026	0.021	0.023
150.75	5.97×10^{-5}	4.44×10^{-3}	5.0	−0.056	0.024	0.026
155.63	5.47×10^{-5}	4.23×10^{-3}	5.0	0.039	0.024	0.026
160.51	5.38×10^{-5}	4.30×10^{-3}	5.0	0.115	0.025	0.027

* relative percentage error
** total error including 0.01 random error

$^{140}Ce(t,t)^{140}Ce$ 17 MeV

θ_{cm}	σ	σ / σ_r	$\Delta\sigma$*	A_y	ΔA_y	ΔA_y**
20.42	1.52×10^{4}	9.51×10^{-1}	5.0	0.000	0.002	0.010
25.53	5.21×10^{3}	7.89×10^{-1}	5.0	0.009	0.002	0.010
30.62	1.70×10^{3}	5.25×10^{-1}	5.0	−0.005	0.011	0.015
35.71	7.59×10^{2}	4.26×10^{-1}	5.0	−0.003	0.011	0.015
40.80	3.75×10^{2}	3.52×10^{-1}	5.0	0.008	0.009	0.013
45.88	2.05×10^{2}	3.01×10^{-1}	5.0	−0.004	0.002	0.010
50.95	9.94×10^{1}	2.16×10^{-1}	5.0	0.004	0.003	0.010
56.02	5.48×10^{1}	1.69×10^{-1}	5.0	0.024	0.004	0.011
61.08	3.27×10^{1}	1.39×10^{-1}	5.0	0.018	0.005	0.011
66.13	1.90×10^{1}	1.07×10^{-1}	5.0	0.019	0.007	0.012
71.17	1.32×10^{1}	9.61×10^{-2}	5.0	0.036	0.008	0.013
76.20	8.14×10^{0}	7.50×10^{-2}	5.0	0.030	0.005	0.011
81.22	4.56×10^{0}	5.20×10^{-2}	5.0	0.058	0.007	0.012
86.24	2.97×10^{0}	4.12×10^{-2}	5.0	0.054	0.008	0.013
91.24	2.39×10^{0}	3.95×10^{-2}	5.0	−0.003	0.009	0.013
96.24	1.73×10^{0}	3.38×10^{-2}	5.0	−0.010	0.009	0.013
101.22	1.02×10^{0}	2.31×10^{-2}	5.0	0.048	0.014	0.017
106.20	6.42×10^{-1}	1.67×10^{-2}	5.0	0.108	0.018	0.021
111.17	5.28×10^{-1}	1.55×10^{-2}	5.0	0.027	0.016	0.019
116.13	5.09×10^{-1}	1.68×10^{-2}	5.0	−0.024	0.013	0.016
121.08	3.66×10^{-1}	1.34×10^{-2}	5.0	−0.012	0.016	0.019
126.02	2.51×10^{-1}	1.01×10^{-2}	5.0	0.063	0.015	0.018
130.95	1.99×10^{-1}	8.66×10^{-3}	5.0	0.077	0.021	0.023
135.88	1.74×10^{-1}	8.18×10^{-3}	5.0	−0.023	0.014	0.017
140.80	1.51×10^{-1}	7.53×10^{-3}	5.0	−0.074	0.020	0.022
145.71	1.28×10^{-1}	6.80×10^{-3}	5.0	−0.008	0.016	0.019
150.62	1.02×10^{-1}	5.68×10^{-3}	5.0	0.067	0.018	0.021
155.52	8.50×10^{-2}	4.92×10^{-3}	5.0	0.082	0.021	0.023
160.42	8.61×10^{-2}	5.16×10^{-3}	5.0	−0.001	0.021	0.023

* relative percentage error
** total error including 0.01 random error

$^{208}Pb(t,t)^{208}Pb$ 17 MeV

θ_{cm}	σ	σ / σ_r	$\Delta\sigma$*	A_y	ΔA_y	ΔA_y**
20.29	3.13×10^{4}	9.71×10^{-1}	5.0	0.006	0.005	0.011
25.35	1.35×10^{4}	1.00×10^{0}	5.0	0.006	0.004	0.011
30.42	6.35×10^{3}	9.69×10^{-1}	5.0	0.005	0.004	0.011
35.48	2.99×10^{3}	8.30×10^{-1}	5.0	−0.001	0.004	0.011
40.54	1.43×10^{3}	6.63×10^{-1}	5.0	0.005	0.003	0.010
45.59	7.47×10^{2}	5.43×10^{-1}	5.0	0.003	0.002	0.010
50.64	3.87×10^{2}	4.17×10^{-1}	5.0	0.001	0.002	0.010
55.68	2.02×10^{2}	3.09×10^{-1}	5.0	0.008	0.002	0.010
60.72	1.20×10^{2}	2.52×10^{-1}	5.0	0.024	0.005	0.011
65.76	7.46×10^{1}	2.09×10^{-1}	5.0	0.017	0.005	0.011
70.79	4.50×10^{1}	1.63×10^{-1}	5.0	0.017	0.005	0.011
75.81	2.75×10^{1}	1.26×10^{-1}	5.0	0.036	0.005	0.011
80.82	1.72×10^{1}	9.77×10^{-2}	5.0	0.048	0.006	0.012
85.83	1.24×10^{1}	8.62×10^{-2}	5.0	0.043	0.006	0.012
90.84	8.68×10^{0}	7.20×10^{-2}	5.0	0.039	0.009	0.013
95.83	5.60×10^{0}	5.47×10^{-2}	5.0	0.061	0.011	0.015
100.82	3.50×10^{0}	3.98×10^{-2}	5.0	0.091	0.011	0.015
105.81	2.60×10^{0}	3.39×10^{-2}	5.0	0.073	0.009	0.013
110.79	2.08×10^{0}	3.08×10^{-2}	5.0	0.065	0.011	0.015
115.76	1.48×10^{0}	2.46×10^{-2}	5.0	0.051	0.011	0.015
120.72	9.74×10^{-1}	1.79×10^{-2}	5.0	0.087	0.015	0.018
125.68	7.03×10^{-1}	1.42×10^{-2}	5.0	0.086	0.018	0.021
130.64	6.10×10^{-1}	1.34×10^{-2}	5.0	0.054	0.018	0.021
135.59	5.35×10^{-1}	1.27×10^{-2}	5.0	0.052	0.013	0.016
140.54	4.21×10^{-1}	1.06×10^{-2}	5.0	0.086	0.015	0.018
145.48	3.11×10^{-1}	8.33×10^{-3}	5.0	0.087	0.016	0.019
150.42	2.61×10^{-1}	7.35×10^{-3}	5.0	0.065	0.019	0.021
155.35	2.35×10^{-1}	6.89×10^{-3}	5.0	0.029	0.022	0.024
160.29	2.24×10^{-1}	6.81×10^{-3}	6.0	0.024	0.021	0.023

* relative percentage error
** total error including 0.01 random error